

## One-pot synthesis of mixed ionic-electronic conducting nanocomposites comprised of fluorite-like and perovskite-like phases as catalytic materials for SOFC

Vladislav Sadykov<sup>1</sup>, Yulia Borchert<sup>1</sup>, Galina Alikina<sup>1</sup>, Anton Lukashevich<sup>1</sup>, Rimma Bunina<sup>1</sup>, Galina Zabolotnaya<sup>1</sup>, Natalia Mezentseva<sup>1</sup>, Ella Moroz<sup>1</sup>, Vladimir Zaikovskii<sup>1</sup>, Dmitrii Zyuzin<sup>1</sup>, Nikolai Uvarov<sup>2</sup>, Vladimir Zyryanov<sup>2</sup>, Nina Orlovskaya<sup>3</sup>.

<sup>1</sup>Boreskov Institute of Catalysis SB RAS, Novosibirsk, Russia

<sup>2</sup>Institute of Solid State Chemistry SB RAS, Novosibirsk, Russia

<sup>3</sup>Dep. Mat. Sci. Eng., Michigan Technological University, Houghton, MI 49931.

### ABSTRACT

Nanocomposites comprised of fluorite-like (doped ceria) and perovskite-like (doped manganite) phases were prepared using a polymerized precursor (Pechini) route and two sources of lanthanides (Ln) - either pure Gd and Ce salts or an industrial ceria-rich mixture of Ln carbonates. Genesis of the structure of composites with annealing temperature has been studied by X-ray diffraction, Transmission Electron Microscopy and Raman. Up to 1300 °C, particle sizes of both fluorite and perovskite phases remain in the nano-range. Nanocomposites possess a high conductivity, lattice oxygen mobility and reactivity with respect to methane exceeding that of individual phases. They are also good catalysts for oxidation of decane by O<sub>2</sub> without coking. Nanocomposite prepared from the industrial Ln source demonstrates better performance than that prepared from pure salts.

### INTRODUCTION

Synthesis of inexpensive mixed ionic - electronic conducting (MIEC) materials, including composites comprised of one electronic conductor and one good ionic conductor is a very important task for design of advanced cathodes and anodes of solid oxide fuel cells (SOFC), oxygen-conducting membranes and sensors [1-7]. The best MIEC composites are obtained by combining gadolinia-doped ceria (CGO) possessing a high ionic conductivity with doped manganites, cobaltites or mixed ferrites-cobaltites of La or Gd. Traditional method of composites preparation by ball-milling a mixture of micron-sized particles of separate phases followed by its pressing and sintering could not guarantee the uniform spatial distribution of components required for a good percolation. Moreover, high (1200-1400 °C or more) temperatures required for sintering often result in phase degradation or formation of isolating interphase boundaries decreasing conductivity and oxygen permeability [3,5,7].

Sintering of nanocrystalline oxides or their composites into dense ceramics is known to proceed at much lower temperatures [8] thus preventing undesired interaction between components. Polymerized precursor (Pechini) route earlier used for synthesis of dense films of nanocrystalline complex oxides [9] and their powders [10, 11] could be applied for synthesis of nanocomposites as well. Due to low equilibrium solubility of Ce<sup>4+</sup> in the perovskites [12] and transition metal (TM) cations in ceria [5, 12], combustion of polyester resin precursor containing lanthanide (Ln) and TM cations in required proportions could produce uniformly intermixed nanoparticles of doped ceria and a perovskite. Such one-pot synthesis of nanocomposites has not been tried up to date, which is the aim of this work. Among TM cations, Mn was selected as being able to activate hydrocarbons in anodes without coking [2]. In the first system with Ce<sub>0.8</sub>Gd<sub>0.2</sub>O<sub>2-x</sub>+GdMnO<sub>3</sub> nominal composition (Ln:Mn=2:1, Ce<sup>4+</sup>:Gd<sup>3+</sup>=2:3) prepared by this route using pure Ln salts (Ce-Gd-Mn), CGO served as proven ionic conductor. Another low cost system attractive for practical applications was prepared using industrially available source of Ln carbonates containing Ce, La, Pr, Nd and Sm. At the same overall Ln:Mn ratio = 2:1 as in the first composite, this second system

differs by the  $\text{Ce}^{4+}:\text{Ln}^{3+}$  ratio  $\sim 3:2$  as well as by the composition of doped ceria phase controlling its ionic conductivity. Structural features, conductivity, oxygen mobility and reactivity of these two systems were estimated and compared.

## EXPERIMENTAL

The mole ratios of citric acid (CA), ethylene glycol (EG) and ethylene diamine (ED) to the total metal ions in the mixed nitrate solution (1.2 M, pH $\sim$ 1) were equal to 3.75:11.25:3.75:1. At a constant stirring, solution of CA in EG was added dropwise at room temperature to the mixed nitrate solution followed by addition of ED. This viscous liquid was evaporated on a hot plate increasing the temperature to 100 °C for 5 h followed by heating at 150 °C for the next 5 h. A solid resin thus formed was burned under air at 500 °C. Powders were pressed in pellets at 15 MPa and calcined at temperatures up to 1300°C with a step of 50-200 °C for 6 hours at each temperature.

All reagents used for synthesis of Ce-Gd-Mn composite were of the “chemical pure grade” (Russia). For synthesis of Ln-Mn composite, a mixed Ln nitrate solution was prepared from the industrial mixture of Ln carbonates supplied by Solikamsk Magnesium Plant, Russia (overall Ln content 50 wt. %, admixtures of Ca, Sr and Na ca 0.8, 0.5 and 0.2 wt.%, resp.; the relative content of La, Ce, Pr, Nd and Sm 25, 60, 5, 9 and 1 wt.%, resp.) by dissolving with required amount of concentrated  $\text{HNO}_3$ .

To compare catalytic properties of perovskite-fluorite nanocomposites and state-of-the-art SOFC anodes in oxidation of hydrocarbons, NiO–ScSZ composite was prepared from NiO (Novamet, US) and 10 mol %  $\text{Sc}_2\text{O}_3$ –1 mol%  $\text{CeO}_2$ –89 mol%  $\text{ZrO}_2$  (ScSZ, DKKK, Japan) powders following procedures described in [13]. The pellets were uniaxially pressed at 15 MPa and sintered at 1150°C for 2 hours.

X-ray diffraction (XRD) patterns were obtained with an URD-6 diffractometer (Germany) using  $\text{Cu K}\alpha$  monochromatic radiation ( $\lambda=1.5418 \text{ \AA}$ ). The  $2\theta$  scanning region was 5-90°. The lattice parameters and particle sizes were obtained using standard procedures [11].

Transmission Electron Microscopy (TEM) micrographs were obtained with a JEM-2010 instrument (lattice resolution 1.4 Å) and acceleration voltage 200 kV. Local elemental analysis was performed with EDX method on Energy-dispersive X-ray Phoenix Spectrometer equipped with Si(Li) detector with energy resolution not worse than 130 eV.

Raman spectra were obtained with a micro-Raman spectrometer Renishaw 1000 using 514.5 nm line of  $\text{Ar}^+$  Ion laser for excitation.

The total electric conductivity of samples was measured in air using a 4284 A Precision LCR Meter. Two silver paste electrodes were used as electrical probes.

The specific surface area ( $S_{\text{sp}}$ ) was determined from Ar thermal desorption data.

The temperature-programmed processes of  $\text{O}_2$  desorption ( $\text{O}_2$  TPD), reduction by  $\text{CH}_4$  ( $\text{CH}_4$  TPR), reoxidation by  $\text{O}_2$  (TPO) and  $\text{C}_{10}\text{H}_{22} + \text{O}_2$  reaction were studied in a flow installation with a quartz reactor and PEM-2M gas analyzer using 0.25-0.5 mm fraction of samples obtained by pellets crushing and grinding [7].

## RESULTS AND DISCUSSION

**XRD.** For samples calcined at temperatures below 850°C, only reflections of a fluorite-like phase (Fig. 1) were observed. For both systems, these phases have increased lattice parameter (Fig. 2) explained by the excess of dissolved big  $\text{Ln}^{3+}$  cations. Indeed, a higher lattice parameter found for Ln-Mn system agrees with a bigger size of  $\text{La}^{3+}$  versus that of  $\text{Gd}^{3+}$  [14]. Decline of the lattice parameter of these metastable phases calcined at 700 °C suggests segregation of  $\text{Ln}^{3+}$  cations. Smaller  $\text{Mn}^{3+/4+}$  cations seem to leave ceria lattice at higher temperatures, which could explain the increase of the lattice parameter for fluorite-like phase in Ce-Gd-Mn system in the 700-850 °C range (Fig. 2). Interaction of these segregated Mn and

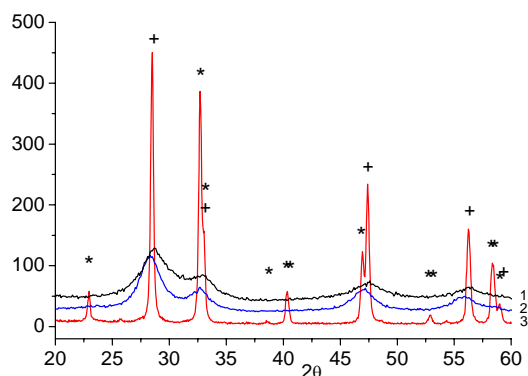


Fig. 1. Diffraction patterns for Ce-Gd-Mn (1) and Ln-Mn (2,3) nanocomposites calcined at 500 °C (1,2) and 1100 °C (3). + fluorite phase, \*- perovskite phase reflections

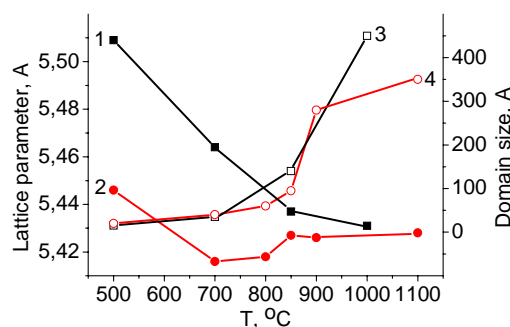


Fig. 2. Dependence of the lattice parameter (1,2) and domain size (3,4) of fluorite-like phases in Ln-Mn (1,3) or Ce-Gd-Mn (2,4) composites on the calcination temperature.

$\text{Ln}^{3+}$  cations generates a perovskite-like phase in samples calcined at  $T \geq 800$  °C. For Ln-Mn system (Fig. 1), this is revealed by appearance of reflections corresponding to pseudocubic  $\text{LaMnO}_3$  phase ( $a=4.04$  Å). For Ce-Gd-Mn system, this phase is of the orthorhombic  $\text{GdMnO}_3$  type (JCPDF-ICDD #25-337,  $a=5.310$ Å,  $b=5.840$ Å,  $c=7.430$ Å). Domain sizes of fluorite-like phases increase with calcination temperature (Fig. 2) remaining in the nanosize range even after 1300 °C, the size of perovskite phase particles being comparable.

**TEM** data for Ce-Gd-Mn composite agree with XRD results giving valuable additional information (Fig. 3). While sample annealed at 500°C is comprised of disordered domains, their size and crystallinity improve after calcinations at 850°C, so high-quality digital diffraction pattern (DDP) is obtained corresponding to  $\text{Ce}_{0.7}\text{Gd}_{0.3}\text{O}_{1.85}$  phase. This suggests a higher content of Gd in doped ceria as compared with the nominal composition (vide supra), and, hence, some Gd deficiency in  $\text{GdMnO}_3$  phase.

In composite annealed at 1100°C, stacking of different phases domains follows the mode perovskite-fluorite-perovskite etc, required for a good percolation (Fig. 4). EDX analysis gives only a traces of Mn in the fluorite-like phase, while similarly only a small (if any) amount of ceria is dissolved in the perovskite structure.

**Raman spectra** (not shown for brevity) for Ln-Mn nanocomposite calcined at 500°C revealed bands at  $\sim 230$ , 450-470 and 540-580  $\text{cm}^{-1}$ . Bands at similar positions are observed for  $\text{LaMnO}_3$  [15], while the band at  $\sim 470$   $\text{cm}^{-1}$  is typical for doped ceria [11]. Hence,  $\text{Ln}^{3+}$  and  $\text{Mn}^{3+/4+}$  cations dissolved in the matrix of disordered metastable fluorite phase exist not only

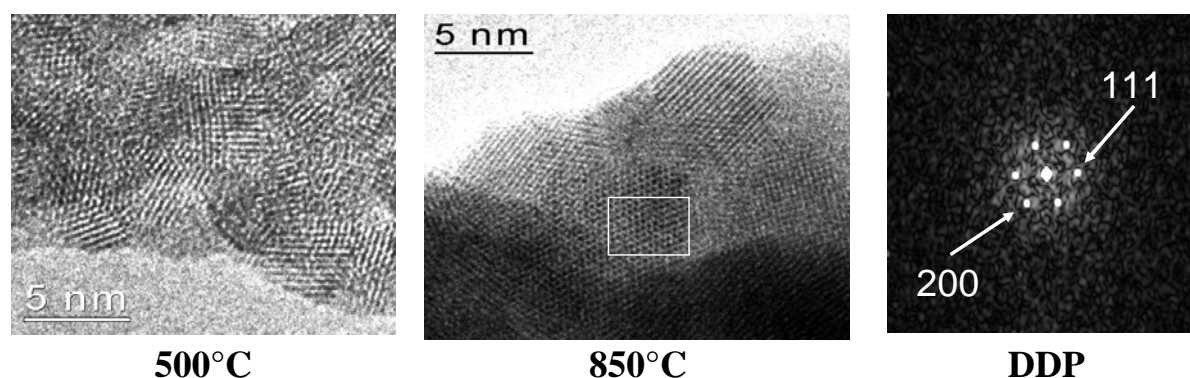


Fig. 3. High resolution TEM images of the lattice of Ce-Gd-Mn nanocomposite annealed at different temperatures and DDP from selected (shown by rectangle) region corresponding to  $\text{Ce}_{0.7}\text{Gd}_{0.3}\text{O}_{1.85}$  phase ( $a=5.431$  Å).

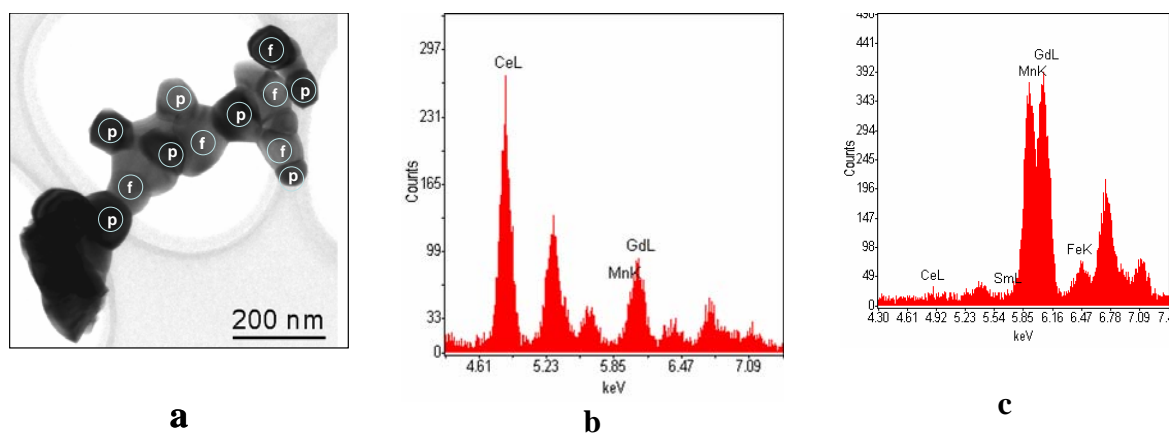


Fig. 4. (a) Typical image of the particle of Ce-Gd-Mn composite annealed at 1100°C with nanodomains of different phases (perovskite-p, fluorite-f) by EDX encircled; (b) and (c) - elemental composition of fluorite and perovskite domains, respectively.

as substitution-type defects (affect lattice parameter, vide supra) but also locally rearrange the lattice forming molecular-scale perovskite-like clusters detected only by Raman.

**Conductivity** (Fig. 5) increases with sintering temperature due to annealing of porosity in pellets and improving percolation. Indeed, the specific surface area decreases from  $\sim 70 \text{ m}^2/\text{g}$  for samples calcined at 500°C to  $\sim 1 \text{ m}^2/\text{g}$  for samples annealed at 1300°C. A higher conductivity for Ln-Mn nanocomposite is due perhaps to some deficiency of  $\text{Ln}^{3+}$  cations (vide supra) leading to a bigger fraction of  $\text{Mn}^{4+}$  cations [10]. For this system, despite dilution of  $\text{LnMO}_3$  in the nanocomposite by doped ceria with a lower conductivity [3,5], the value of the total conductivity extrapolated to 1000 K ( $\sim 15 \text{ S/cm}$ ) is rather close to that reported for porous Ca, Sr-doped  $\text{LaMnO}_3$  ( $\sim 50\text{-}70 \text{ S/cm}$ ) [3, 12] or Gd-Sr(Ca) $\text{MnO}_3$  ( $10\text{-}30 \text{ S/cm}$ ) [16]. This value is also either close to typical values of conductivity of perovskite/fluorite composites such as La-Sr-Mn/Ce-Gd ( $30\text{-}50 \text{ S/cm}$ ) [3] or even higher than that for such MIEC composites as  $\text{Ce}_{0.8}\text{Gd}_{0.2}\text{O}_{1.9}/\text{Gd}_{0.7}\text{Ca}_{0.3}\text{CoO}_{3-\delta}$  ( $\sim 10^{-2} \text{ S/cm}$ ) [5] or  $\text{La}_{0.6}\text{Sr}_{0.2}\text{Ca}_{0.1}\text{Bi}_{0.1}\text{Ga}_{0.6}\text{Mg}_{0.1}\text{Zn}_{0.1}\text{Fe}_{0.2}\text{O}_{3-x}/\text{La}_{0.4}\text{Ca}_{0.4}\text{Bi}_{0.2}\text{Mn}_{0.6}\text{Fe}_{0.4}\text{O}_{3-x}$  ( $\sim 10^{-1} \text{ S/cm}$ ) [7]. For Ln-Mn system, the level of conductivity also falls within the range of  $10^{-1}$  -40 S/cm typical for potential oxide anodes [2]

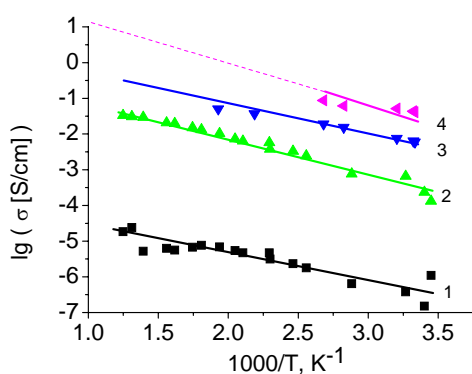


Fig. 5. Temperature dependence of conductivity for Ce-Gd-Mn (1-2) and Ln-Mn (3-4) nanocomposites sintered at 900 (1,3) and 1300 (2,4) °C.

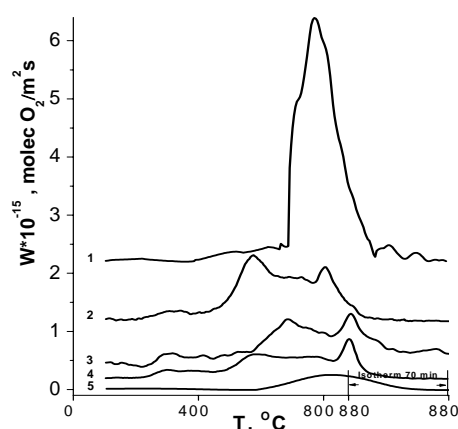


Fig. 6. TPD  $\text{O}_2$  for Ln-Mn (1-3) and Ce-Gd-Mn (4, 5) nanocomposites sintered at 1100 (1, 5), 500 (2,4) and 900 (3) °C. For curve 5, rates were multiplied by 10.

**O<sub>2</sub> TPD** curves (Fig. 6) demonstrate close positions of main peaks for both types of systems calcined at 500°C, higher desorption rates being observed for Ln-Mn system. Annealing at 1100°C increases the rate of oxygen desorption from Ln-Mn nanocomposite, while strongly decreasing it for Ce-Gd-Mn. Since high-temperature oxygen desorption from doped La manganite is controlled by the oxygen mobility in the bulk of particles [10, 17], this implies that complexity of the chemical composition of both fluorite-like and perovskite-like phases in Ln-Mn system facilitates the oxygen mobility, probably via disordering both domains and domain boundaries. From the practical point of view, less expensive Ln-Mn nanocomposite with a higher oxygen mobility is more promising for SOFC cathodes.

**CH<sub>4</sub> TPR.** Typical CH<sub>4</sub> TPR curves (Fig. 7a) contain middle-temperature peaks of CO<sub>2</sub> evolution (CH<sub>4</sub> combustion) along with CO and H<sub>2</sub> peaks at higher temperatures (CH<sub>4</sub> selective oxidation by the lattice oxygen). Specific peak rates (Fig. 7b) controlled by the lattice oxygen mobility [10, 11] tend to increase with sintering temperature correlating with the increase of conductivity (Fig.5). For nanocomposites sintered at high temperatures, the peak rates of the oxygen consumption along both combustion and selective oxidation routes exceed by an order of magnitude corresponding rates for pure or doped lanthanum manganite and ferrites [10] or Gd/Pr-doped ceria even promoted by Pt [11]. This feature clearly demonstrates that Mn cations in nanocomposites efficiently activate methane even at middle temperatures, while a plenty of domain/interphase boundaries ensure a high flux of the lattice oxygen to the surface during reduction by CH<sub>4</sub>.

**Catalytic activity.** In the C<sub>10</sub>H<sub>22</sub>+ O<sub>2</sub> reaction at short contact times, both nanocomposites demonstrate a good performance even in the middle-temperature range, where NiO–ScSZ composite is inactive (Fig. 8). A higher activity of Ln-Mn nanocomposite agrees with a higher lattice oxygen mobility and reactivity (Figs. 6, 7). No deterioration of performance with time on- stream was observed (see isothermal part of the run for 70 min at 880 °C, Fig. 8). TPO after this run revealed no carbon deposition for nanocomposites, while up to 120 monolayers of carbon was revealed for NiO–ScSZ state-of-the-art composite. Nanocomposites were also found to be efficient in the steam reforming of decane ensuring at contact times ~ 0.1 s equilibrium composition of the stoichiometric C<sub>10</sub>H<sub>22</sub> +H<sub>2</sub>O feed at temperatures ~ 700°C (not shown for brevity). Hence, these nanocomposites could be promising as components of SOFC

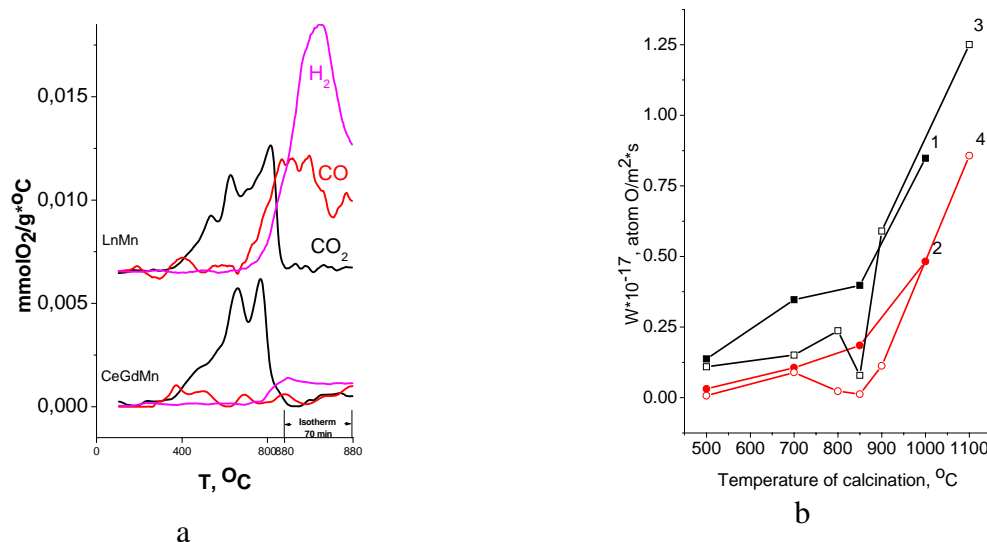


Fig. 7. Typical CH<sub>4</sub> TPR curves for Ln-Mn and Ce-Gd-Mn composite sintered at 850°C (a); peak rates of CH<sub>4</sub> transformation into deep (1,3) and partial (2,4) oxidation products by the lattice oxygen for Ln-Mn (1,2) and Ce-Gd-Mn (3,4) composites. Feed 1% CH<sub>4</sub> in He, temperature ramp 5°/min.

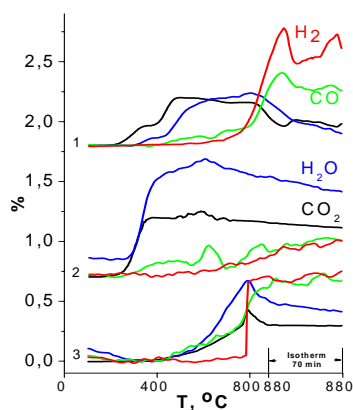


Fig. 8. Typical curves of products formation during temperature-programmed  $C_{10}H_{22} + O_2$  reaction on Ce-Gd-Mn (1) and Ln-Mn (2) composites sintered at  $500^\circ C$  as compared with performance of NiO-ScSZ (3) composite. Feed composition 0.1%  $C_{10}H_{22} + 0.5\%$   $O_2$  in He, contact time 3 ms, pretreatment in  $O_2$  at  $500^\circ C$  for 2 h before reaction.

anodes operating on direct oxidation or steam reforming of long-chain hydrocarbons, having such additional advantage versus complex perovskites [2] as a lower thermal expansion.

## CONCLUSIONS

Polymerized precursor (Pechini) route allows to obtain mixed ionic-electronic conducting nanocomposites comprised of perovskite (doped lanthanum manganite) and fluorite (doped ceria) phase through one-pot procedure using either pure salts or an inexpensive industrial mixture of lanthanides for synthesis. These systems, especially more complex one with a lower cost, possess conductivity, lattice oxygen mobility and reactivity as well as catalytic activity in decane oxidation by  $O_2$  promising for their application as advanced materials for SOFC and catalytic MIEC membranes.

**Acknowledgements.** This work is in part supported by NATO SFP 980878 and ISTC 3234 Projects.

## REFERENCES

1. V. Dusastre, J.A. Kilner, *Solid State Ionics* **126**, 163 (1999)
2. A. Atkinson, S. Barnett, R.J. Gorte et al, *Nat. mater.* **3**, 17 (2004).
3. V.V. Kharton, A.V. Kovalevsky, A.P. Biskup et al, *Solid State Ionics* **160**, 247 (2003).
4. F.M. Figueiredo, J.R. Frade, F.M.B. Marques, *Solid State Ionics* **135**, 463 (2000).
5. U. Nigge, H.-D. Wiemhofer, E.W.J. Romer, H.J.M. Bouwmeester, T.R. Schulte, *Solid State Ionics* **146**, 163 (2002).
6. E. Perry Murray, S.A. Barnett, *Solid State Ionics* **143**, 265 (2001).
7. V.V. Zyryanov, N.F. Uvarov, V.A. Sadykov et al, *Catal. Today* **104**, 114 (2005).
8. I. Kosacki, T. Suzuki, V. Petrovskii, H.U. Anderson, *Solid State Ionics* **136**, 1225 (2001).
9. M. P. Pechini: U.S. Patent 3,330,697 (1967).
10. V. A. Sadykov, N. N. Bulgakov, V. S. Muzykantov, et al, in: "Mixed Ionic Electronic Conducting Perovskites for Advanced Energy Systems", (N.Orlovskaya, N. Browning Eds.), Kluwer Academic Publ., Boston/Dordrecht/London, 2004, P. 49-70.
11. V. A. Sadykov, S.N. Pavlova et al, *Kinetics and Catalysis* **46**, 227 (2005).
12. M. Mori, Y. Hiei, T. Yamamoto, H. Itoh, *J. Electrochem. Soc.* **146**, 4041 (1999).
13. H. Kishimoto, T. Horita, K. Yamaji, Y. Xiong, et al, *Solid State Ionics* **175**, 107 (2004).
14. R. D. Shannon, *Acta Cryst. A* **32**, 751 (1976).
15. C. Roy, R.C. Budhani, *J. Appl. Phys.* **86**, 3125 (1999).
16. H.Y. Tu, M.B. Phillips, Y. Takeda et al, *J. Electrochem. Soc.* **146**, 2085 (1999).
17. T. Bak, J. Nowotny, M. Rekas, C.C. Sorrell, E.R. Vance, *Solid State Ionics* **135**, 557 (2000).